

## Article

# Investigation on the Sensitivity of Precipitation Simulation to Model Parameterization and Analysis Nudging over Hebei Province, China

Yuanhua Li <sup>1</sup>, Zhiguang Tian <sup>1</sup>, Xia Chen <sup>2,3</sup>, Xiashu Su <sup>4,5</sup> and Entao Yu <sup>5,6,\*</sup> 

<sup>1</sup> Hebei Meteorological Information Center, Shijiazhuang 050021, China; hbsqxjlyh@sina.com (Y.L.); hbsqxjlyh@aliyun.com (Z.T.)

<sup>2</sup> Hebei Climate Center, Shijiazhuang 050021, China; chenxia1218@sina.com

<sup>3</sup> Hebei Key Laboratory for Meteorology and Eco-Environment, Shijiazhuang 050021, China

<sup>4</sup> School of Ecology and Environment, Inner Mongolia University, Hohhot 010021, China; suxiashu@163.com

<sup>5</sup> Nansen-Zhu International Research Centre, Institute of Atmospheric Physics, Chinese Academy of Sciences, Beijing 100029, China

<sup>6</sup> Collaborative Innovation Center on Forecast and Evaluation of Meteorological Disasters (CIC-FEMD), Nanjing University of Information Science & Technology, Nanjing 210044, China

\* Correspondence: yuet@mail.iap.ac.cn

**Abstract:** The physical parameterizations have important influence on model performance in precipitation simulation and prediction; however, previous investigations are seldom conducted at very high resolution over Hebei Province, which is often influenced by extreme events such as droughts and floods. In this paper, the influence of parameterization schemes and analysis nudging on precipitation simulation is investigated using the WRF (weather research and forecasting) model with many sensitivity experiments at the cumulus “gray-zone” resolution (5 km). The model performance of different sensitivity simulations is determined by a comparison with the local high-quality observational data. The results indicate that the WRF model generally reproduces the distribution of precipitation well, and the model tends to underestimate precipitation compared with the station observations. The sensitivity simulation with the Tiedtke cumulus parameterization scheme combined with the Thompson microphysics scheme shows the best model performance, with the highest temporal correlation coefficient (0.45) and lowest root mean square error (0.34 mm/day). At the same time, analysis nudging, which incorporates observational information into simulation, can improve the model performance in precipitation simulation. Further analysis indicates that the negative bias in precipitation may be associated with the negative bias in relative humidity, which in turn is associated with the positive bias in temperature and wind speed. This study highlights the role of parameterization schemes and analysis nudging in precipitation simulation and provides a valuable reference for further investigations on precipitation forecasting applications.

**Keywords:** precipitation simulation; Heibe Province; model parameterization; analysis nudging



**Citation:** Li, Y.; Tian, Z.; Chen, X.; Su, X.; Yu, E. Investigation on the Sensitivity of Precipitation Simulation to Model Parameterization and Analysis Nudging over Hebei Province, China. *Atmosphere* **2024**, *15*, 512. <https://doi.org/10.3390/atmos15040512>

Academic Editor: Muhammad Jehanzaib

Received: 29 March 2024

Revised: 18 April 2024

Accepted: 18 April 2024

Published: 22 April 2024



**Copyright:** © 2024 by the authors. Licensee MDPI, Basel, Switzerland. This article is an open access article distributed under the terms and conditions of the Creative Commons Attribution (CC BY) license (<https://creativecommons.org/licenses/by/4.0/>).

## 1. Introduction

The atmosphere is a complex system characterized by nonlinear interactions across wide scales [1,2], including planetary waves, synoptic systems, secondary circulations, mesoscale systems, turbulent eddies, cloud microphysics, and molecular diffusion. The mathematical representation of these atmospheric phenomena in numerical models is often streamlined, depending on the model’s intended purpose, resolution, and emphasis [3]. The dynamical core of the weather prediction model effectively solves the governing equations within a discretized grid, neglecting terms of relative insignificance. Unresolved physical elements, such as radiation, deep and shallow cumulus convection, cloud microphysics, precipitation, and turbulence, are always represented by parameterization in models [4–9].

In meteorological models, the horizontal grid spacing ranging approximately from 3 to 10 km is often called the convective gray-zone resolution (hereinafter referred to as gray-zone resolution). In this resolution, the model can identify organized mesoscale convective systems, while it cannot resolve individual convective cells; thus, this grid spacing lacks the precision to represent distinct convective features, yet it is too detailed for convective parameterizations [10–14]. Previous studies indicate that simulations at gray-zone resolution reproduce fewer convective clouds; they succeed in reproducing the statistical characteristics of convection [15–17]. Thus, simulations at the gray-zone resolution are a valuable and cost-effective methodology for investigating the impact of convection in regional climate models [11,12,18–21].

Among the complex atmospheric processes influencing precipitation simulation, convective cumulus parameterization schemes play a crucial role [22,23], which serve the purpose of representing sub-grid scale convective processes that elude explicit resolution. These schemes are designed to encapsulate the vertical transport phenomena, including the heat, moisture, and momentum associated with convective clouds, thereby influencing the precipitation simulation.

A lot of previous studies investigated the sensitivity of precipitation to the choice of cumulus parameterization schemes; for example, in simulating heavy rainfall events for the Indian monsoon region using the WRF model, the Betts Miller Janjic (BMJ) cumulus scheme outperformed other schemes [24], while the Kain–Fritsch (KF) cumulus scheme indicated the best performance in simulating precipitation for three flood events in Alberta, Canada [25]. The study over the Basque Country of Spain indicated that the KF scheme yielded superior results in simulating extreme precipitation events compared to other available cumulus schemes [26]. Other studies indicated that the model sensitivity to the cumulus schemes is more pronounced compared with that to the initial conditions [27], and it was particularly notable in the higher resolution simulations [28]. At the same time, the microphysics schemes, which deal with cloud microphysical processes, such as moisture evaporation and condensation, can change thermodynamic and dynamic interactions in the atmosphere and influence the precipitation simulation.

Hebei Province in China has distinctive climatic features, characterized by the monsoonal influences, mountainous topography, and urbanization, and the precise forecasting of precipitation poses a great challenge [29–31]. Previous studies have explored the impact of cumulus schemes on precipitation simulations at a resolution of approximately 20–30 km. It is imperative to ascertain the most effective physical parameterization schemes tailored to high-resolution precipitation variations to enhance forecast performance for precipitation at regional or local scales, and these studies can identify the optimal combinations of physical parameterization schemes for precipitation forecasting. In this study, as an initial investigation on the influence of physical parameterizations on the model performance on precipitation simulations, several sensitivity experiments with different model configurations, such as the cumulus scheme, the microphysical scheme, and analysis nudging, were conducted using the WRF model at a cumulus gray-zone resolution of 5 km, which will help determine the best model configuration for precipitation simulations, subsequently improving the precipitation forecasting over this region.

## 2. Materials and Methods

In this study, the Advanced Research WRF (WRF-ARW) version 4.5.1 was employed. The WRF model is a simulation system that was designed for both atmospheric research and operational forecasting applications [32].

The simulation domain of the WRF model is illustrated in Figure 1, locating in North China with a horizontal grid spacing of 5 km. Vertically, the WRF model is structured with the model top set at 50 hPa and 51 levels, utilizing a terrain-following, hydrostatic-pressure vertical coordinate. The initial and boundary conditions are from ERA5 reanalysis dataset, which is a newly developed reanalysis product by the European Centre for Medium-range Weather Forecasts and offers a comprehensive record of the global atmosphere, land surface,

and ocean waves [33]. This dataset is widely used as forcing dataset for regional climate simulation over China [18,21,34].

### Topography of the WRF simulation Domain

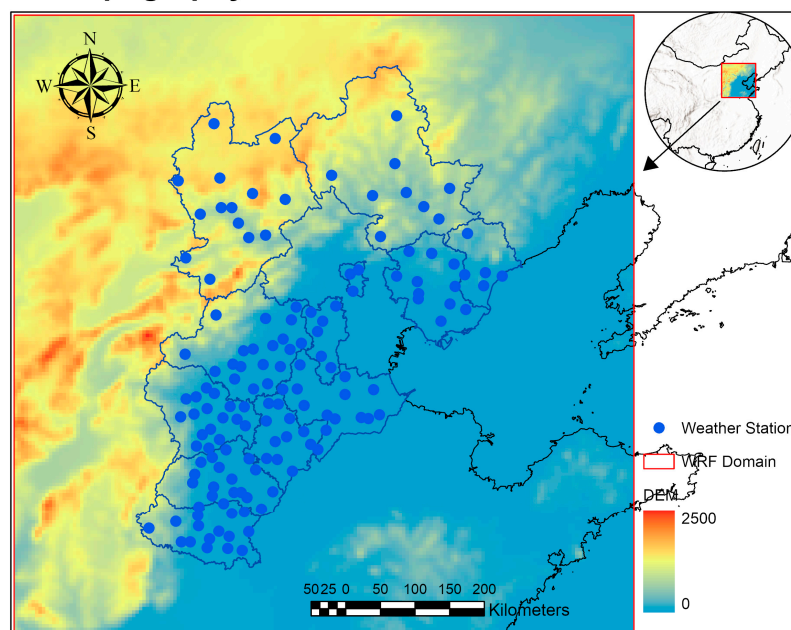


**Figure 1.** Model domain with topography (unit: meters), blue solid circles represent the observational stations (142 stations in total), and the location of simulation domain is illustrated at top right of the figure.

Table 1 lists the physical parameterization schemes used in the sensitivity simulations, with a total of seven sensitivity experiments conducted. Among them, two microphysics schemes, including the WRF single-moment 6-class (WSM6) scheme [35] and the Thompson scheme [36], and two cumulus convective schemes, including the Kain–Fritsch scheme [37] and Tiedtke scheme [38], were used. The first four sensitivity experiments (Run1–Run4) were configured with different combinations of cumulus and microphysical schemes. Given the horizontal grid spacing of 5 km falls in the cumulus “gray-zone” resolution, two experiments (Run5 and Run6) were configured with the cumulus convective schemes turning off. Furthermore, a sensitivity experiment with analysis nudging (Run7) was configured to investigate its effects on model simulation. Analysis nudging is a grid-based four-dimensional data assimilation technique nudging the model toward data analysis. The model is run with extra nudging terms for horizontal winds, temperature, and water vapor. These terms nudge point by point to a three-dimension space- and time-interpolated analysis field [32,39]. Analysis nudging improves the model ability by incorporating observational information into simulation; thus, it should be clarified that the inclusion of analysis nudging in WRF experiments could serve the more accurate estimation of the fallen area mean precipitations but not precipitation forecasts. Except the physical schemes listed in Table 1, the model configuration of the sensitivity experiments was identical, including the Yonsei University (YSU) scheme [40], the Rapid Radiative Transfer Model longwave radiation scheme [41], the Dudhia shortwave radiation scheme [42], and the community Noah land surface model with multi-parameterization options [43,44].

**Table 1.** Model physics parameterization schemes for each sensitivity experiment.

Name	Cumulus Scheme	Microphysical Scheme	Analysis Nudging
Run1	KF	WSM6	\
Run2	KF	Thompson	\
Run3	Tiedtke	WSM6	\
Run4	Tiedtke	Thompson	\
Run5	\	WSM6	\
Run6	\	Thompson	\
Run7	KF	WSM6	Yes

As an initial attempt to explore the differences of model performance in reproducing the precipitation over Hebei Province, which will be helpful in understanding the influence of parameterization schemes on precipitation simulation and selecting the best model configuration for further precipitation forecast application, we chose a whole summer month of July 2017 as the case study period. It is true that for obtaining generally valid conclusions for a given area such as Hebei Province, much longer simulation period instead of one month or one year should be performed; however, the high resolution and consequent small time step require large amount of computational resources for a single sensitivity simulation. Due to the limitation of computational resources, one month simulation period was acceptable in this study, and the results were meaningful to the following application studies. All sensitivity simulations were carried out from 30 June to 31 July 2017, incorporating a 2-day reinitialization period to prevent model drift. Each reinitialization involved a 72 h simulation, along with the first 24 h simulations designated as the spin-up period.

The performances of different sensitivity simulations were determined by comparison of the simulated meteorological variables with the dense station observations over Hebei Province. The observational variables included precipitation, temperature at 2 m, relative humidity at 2 m, and wind speed at 10 m. For the model simulation, the results of the model grids that were geographically closest to the station observations were selected. It is true that in model and observation comparison, the discrepancies arising from non-overlapping is evident, and although some uncertainties may have been introduced during the comparison in this study, these uncertainties were consistent in all the sensitivity experiments; thus, they could be ignored in the comparison and will not change the results of this study. Thus, the flowchart of the methodology in this study can be summarized in Figure 2.

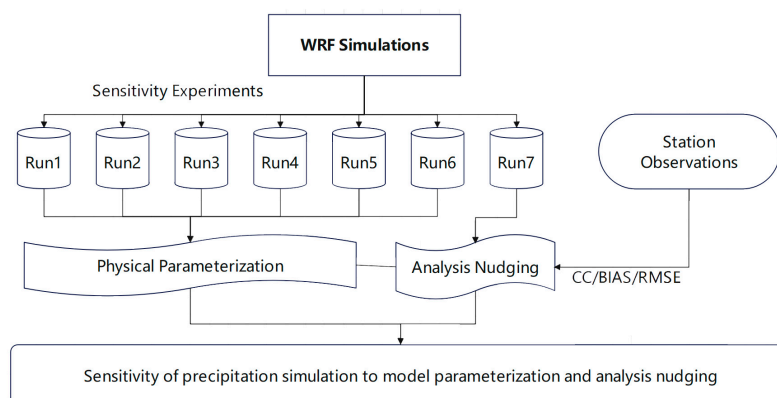


**Figure 2.** The flowchart of methodology in this study.

Three commonly used metrics in previous model evaluation studies, including the Pearson correlation coefficient (*CORR*), *BIAS*, and root mean square error (*RMSE*), were used to evaluate the performances of the model simulations. These statistical scores measure the agreement between simulation and observations and are important in evaluating

the performance. Applying these commonly used metrics can also provide references for other evaluation studies using the WRF model. *CORR*, *BIAS*, and *RMSE* measure the performance in different perspectives. *CORR* indicates the strength as well as the direction of linear relationship between the station observation and model simulation, while *BIAS* measures the deviation between observation and simulation. *RMSE*, on the other hand, measures the square root of average of variances between observation and simulations. There are also other metrics, such as R square and relative bias, that can be used; however, they serve the same purpose. Thus, in this study, only these metrics were applied to provide the measurement of performance of the sensitivity simulations.

The definitions of these metrics are as follows:

$$CORR = \frac{\sum_{i=1}^N (M_i - \bar{M})(O_i - \bar{O})}{\sqrt{\sum_{i=1}^N (M_i - \bar{M})^2 \cdot \sum_{i=1}^N (O_i - \bar{O})^2}} \quad (1)$$

$$BIAS = \frac{1}{N} \sum_{i=1}^N (M_i - O_i) \quad (2)$$

$$RMSE = \sqrt{\frac{1}{N} \sum_{i=1}^N (M_i - O_i)^2} \quad (3)$$

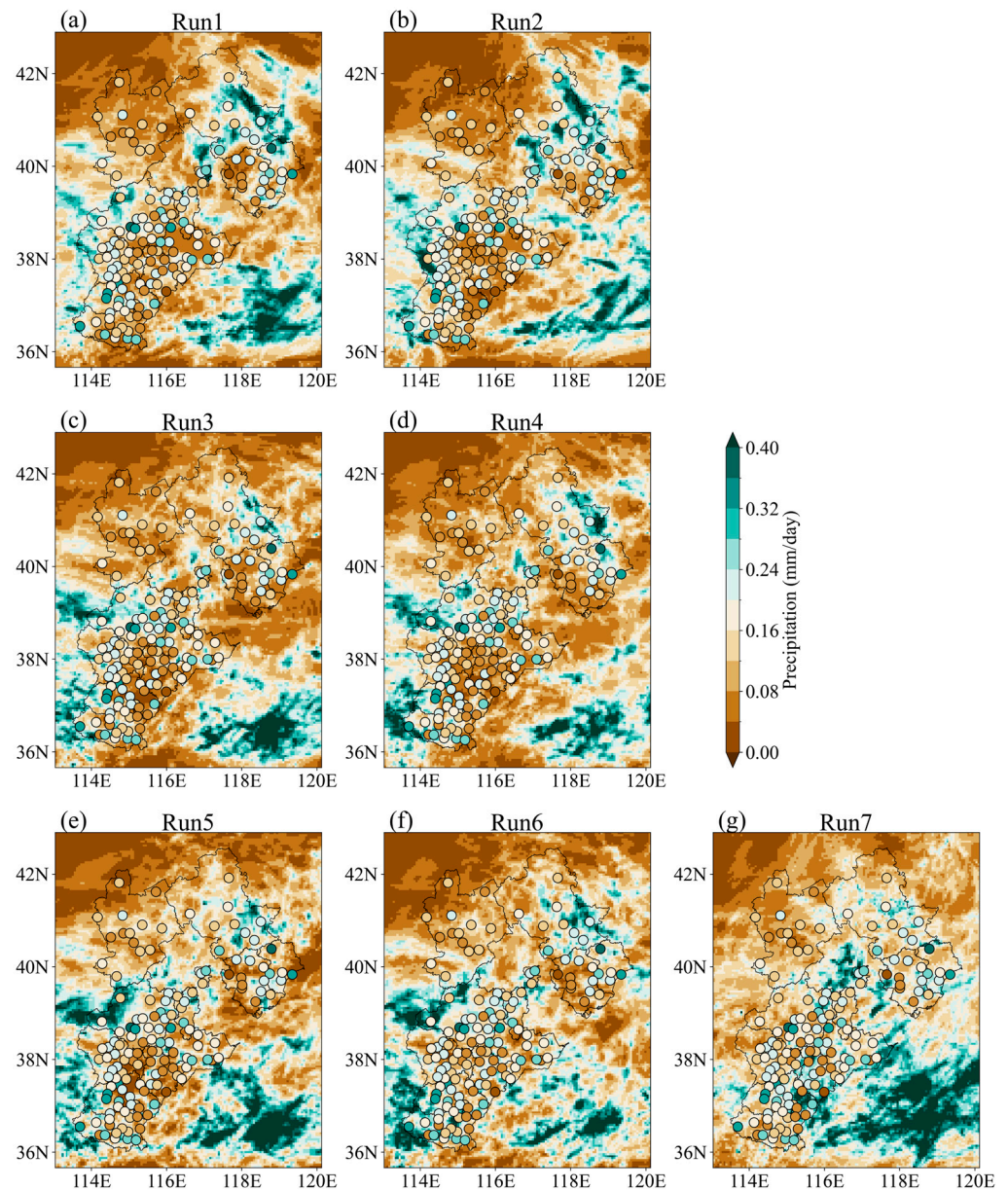
Here,  $M$  is the value of the model output,  $O$  is the value of the observation, and  $N$  is the number of observations.

### 3. Results

Figure 3 illustrates the spatial distribution of the mean precipitation for the sensitivity experiments alongside the corresponding observations. The WRF simulations generally capture the spatial features of precipitation over Hebei Province, including more precipitation over the western and central regions characterized by complicated topography (Figure 1). However, nearly all sensitivity experiments underestimate precipitation compared to station observations, especially over the southwestern regions. Notably, simulations employing the Kain–Fritsch scheme (Run1 and Run2) generate higher precipitation across the simulation domain compared to those using the Tiedtke cumulus scheme (Run3 and Run4). Interestingly, the simulations with cumulus schemes turning off (Run5 and Run6), the same as the Kain–Fritsch scheme, yield more precipitation compared to the Tiedtke scheme, resulting in reduced underestimation and an improved agreement with observations.

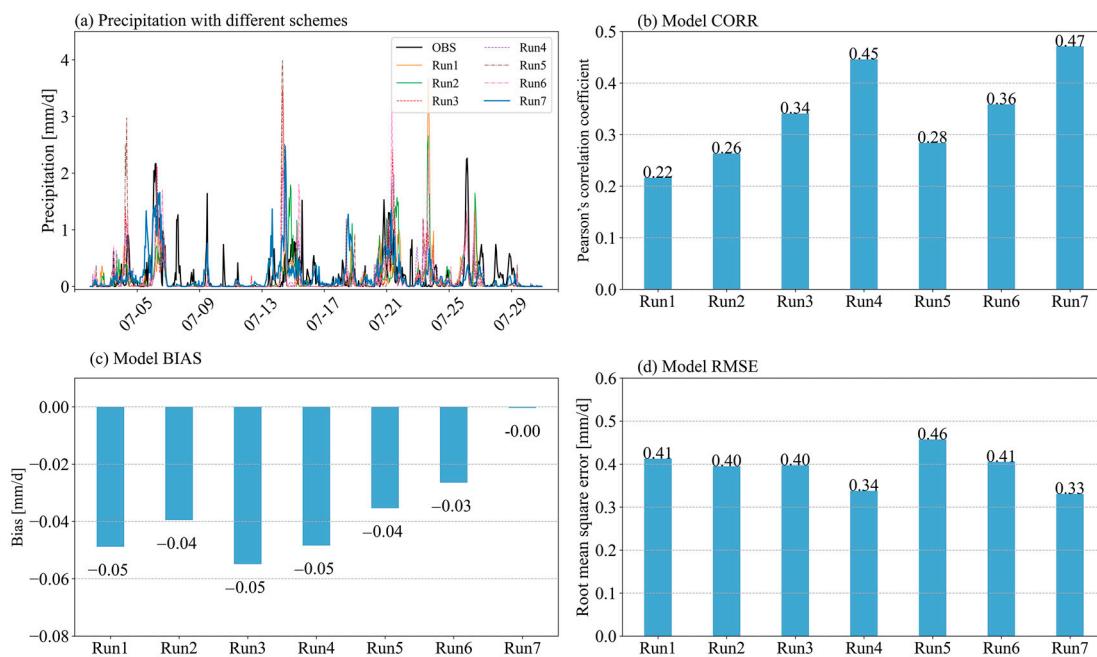
Regarding microphysics schemes, the Thompson scheme (Run2, Run4, and Run6) tends to produce more precipitation over Hebei Province compared to the WSM6 scheme (Run1, Run3, and Run5). Analysis nudging, in particular, improves the model simulation significantly, as Run7 reproduces the features of observational precipitation well, in both spatial distribution and amount. For most of the stations, the simulated precipitation of Run7 and observed quantities are fairly comparable, which is likely due to the continuous nudging towards the observed atmospheric conditions that helps to maintain the consistency with real-world observations throughout the simulation period.

Figure 4 represents the time series of average precipitation for both observation and model simulations. For the observation, the average precipitation was calculated by the mean of precipitation for all 142 stations, while for the simulation, we first selected the simulation results of the grid points that are geographically closest to the weather stations, then calculated the precipitation average. This kind of comparison between the observation and simulation may have some error; however, they are consistent for all the stations and the sensitivity experiments and thus will not change the results of this study. Overall, WRF can reproduce the time series of precipitation, capturing the majority of precipitation events occurring over Hebei Province. For instance, the precipitation events on 6 July and 26 July are well reproduced by most of the sensitivity runs. At the same time, most of the WRF simulations overestimate the precipitation events on 14 July and 24 July while underestimating those on 8 and 10 July.



**Figure 3.** Comparison of daily mean precipitation of July 2017 between observational data (colored dots) and sensitivity simulations (shadings). Units: mm/day.

In contrast, analysis nudging shows an overall improvement compared to other experiments, particularly evident in the events on 10 July, 14 July, and 21–22 July. In consequence, the *BIAS* scores of the parameterization scheme runs (Run1 to Run6) range from  $-0.05$  to  $-0.03$  mm/day, whereas for the analysis nudging experiment (Run7), the *BIAS* approaches zero (Figure 4c). Furthermore, among the parameterization scheme experiments, the simulation employing the Tiedtke and Thompson scheme (Run4) achieves the highest *CORR* (0.45) and lowest *RMSE* (0.34 mm/day), which can be considered as the best choice for precipitation simulation over Hebei Province. Moreover, the analysis nudging shows even higher scores of *CORR* (0.47) and *RMSE* (0.33 mm/day), highlighting the benefits of applying analysis nudging techniques in WRF prediction.

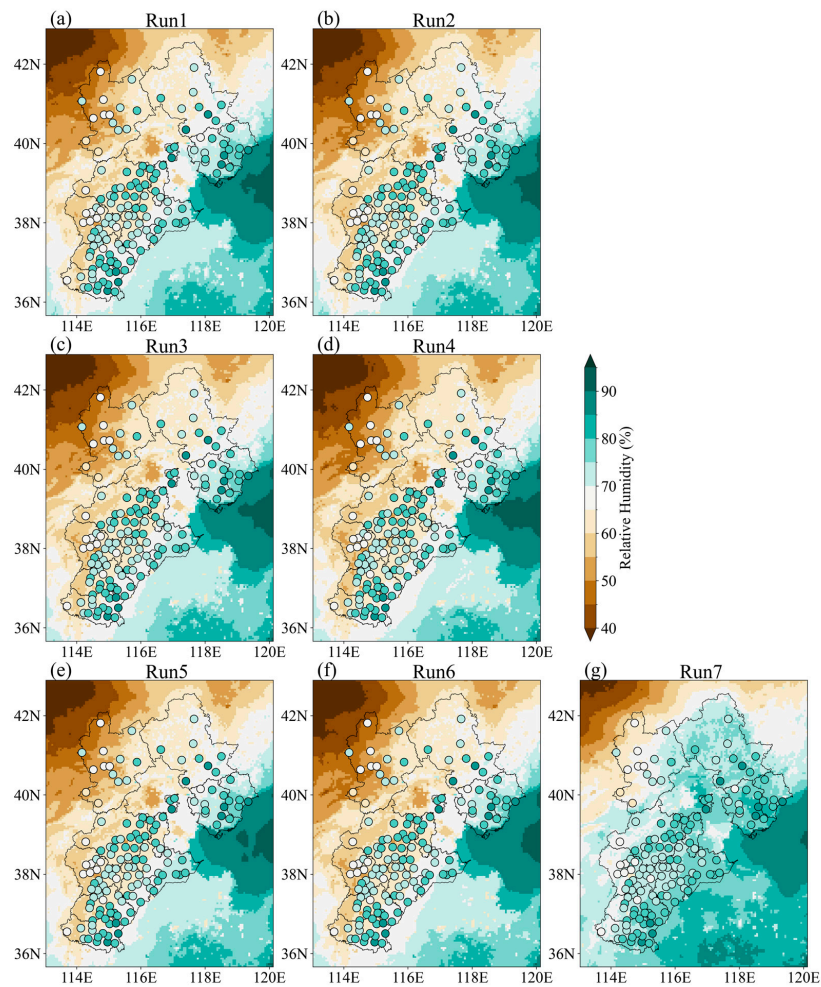


**Figure 4.** The time series of daily precipitation averaged of all station observations and that of the corresponding sensitivity simulations (a) as well as the statistical scores of *CORR* (b), *BIAS* (c), and *RMSE* (d) for the sensitivity experiments.

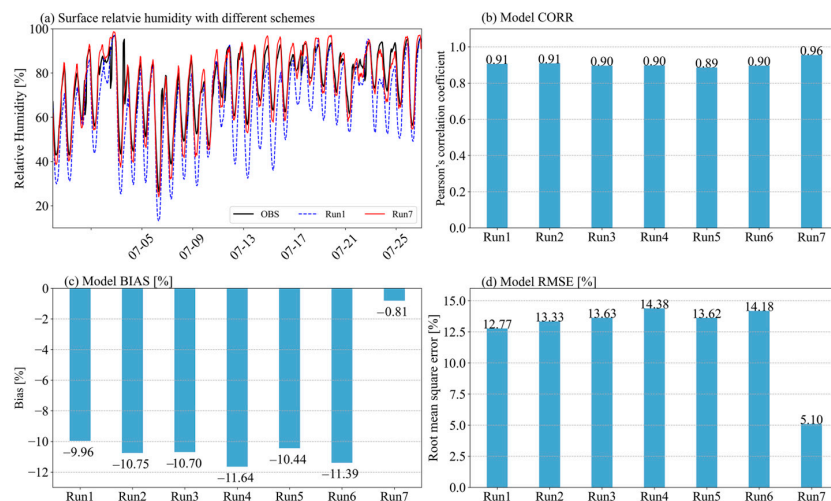
The spatial distribution of observational and simulated surface relative humidity is illustrated in Figure 5, given its significant influence on precipitation. All WRF simulations reasonably reproduce the decreasing trend from southeast to northwest across Hebei Province, which is consistent with the observations. At the same time, all the sensitivity simulations tend to underestimate the relative humidity compared to the observation; it is particularly clear in the western and central regions of Hebei Province, which is consistent with the bias of precipitation (Figure 3). The spatial distribution of relative humidity simulated by different parameterization schemes are very similar; thus, the model biases are also quite similar. Notably, the simulation with analysis nudging (Run7) shows distinct improvement compared to other simulations, as it produces much higher relative humidity over the simulation domain, which reduces the model bias and shows better agreement with the observations, especially over the central regions of Hebei Province.

Figure 6 shows the time series of relative humidity from observations and sensitivity simulations. The diurnal cycle of relative humidity can be well reproduced by all the simulations, while almost all parameterization scheme experiments tend to underestimate relative humidity during the daytime hours. Conversely, simulations generally show good agreement with observations during nighttime periods. The differences between the physical scheme experiments are quite minimal, reflected in the statistical metrics of *CORR*, *BIAS*, and *RMSE*. According to the statistical scores, the simulation employing the Kain–Fritsch and WSM6 schemes ranks first among the experiment, with the highest *CORR* (0.91) alongside the lowest *BIAS* (−9.96%) and *RMSE* (12.77%).

However, analysis nudging significantly improve the model simulations, being evident not only in the time series but also in the statistical metrics. The experiment with analysis nudging (Run7) reproduces the time series of relative humidity for both daytime and nighttime periods well, yielding the best scores in *CORR* (0.96), *BIAS* (−0.81%), and *RMSE* (5.10%). This significant improvement may be attributed to the direct nudging of relative humidity during the model simulation; conversely, precipitation is not assimilated during the model simulation.



**Figure 5.** Comparison of daily mean surface relative humidity of July 2017 between the observational data (colored dots) and sensitivity simulations (shadings). Units: %.



**Figure 6.** The time series of surface relative humidity averaged across all station observations, alongside those of the corresponding sensitivity simulations (a) as well as the statistical scores of CORR (b), BIAS (c), and RMSE (d) for the sensitivity experiments.

Figure 7 shows the spatial distribution of the average surface temperature from station observations and model simulations; the WRF model with different physical parameteriza-

tion schemes generally reproduces the spatial features of temperature, while significant overestimations are observed in the model simulations. The simulations with different physical parameterization schemes are very similar, indicating that cumulus and micro-physical schemes have a small effect on the temperature simulation. However, analysis nudging improves the simulation by reducing the overestimation of temperature, and the simulation of Run7 shows better agreement with the station observations.

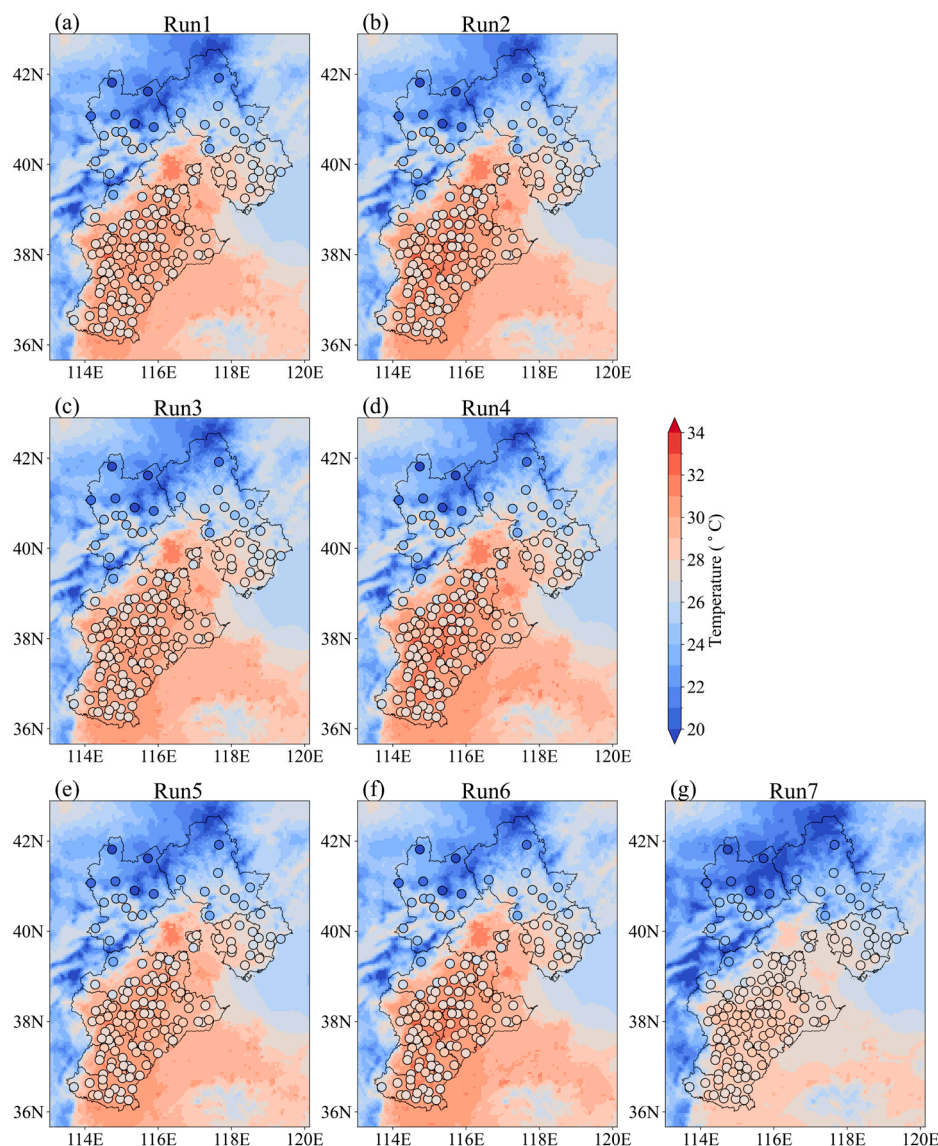


**Figure 7.** Comparison of daily mean temperature in July 2017 between the observational data (colored dots) and sensitivity simulations (shadings). Units:  $^{\circ}\text{C}$ .

Figure 8 illustrates the time series of temperature averaged across all stations and the results of corresponding sensitivity experiments. While the WRF model reproduces the diurnal cycle of temperature well, it shows significant overestimation during the daytime hours, which is consistent with the overestimation in Figure 7. Conversely, WRF reproduces the temperature at nighttime periods well, with good agreement with the observations. Notably, simulation with analysis nudging shows much better performance in reproducing the time series of temperature, with better agreement with observation throughout both nighttime and daytime periods. Consequently, the statistical score of the *BIAS* of the analysis nudging experiment (Run7) is  $0.35^{\circ}\text{C}$ , which is significantly lower than the other sensitivity experiments ( $2.21\sim 2.70^{\circ}\text{C}$ ). Regarding the parameterization

scheme experiments, the simulation with Kain–Fritsch and WSM6 (Run1) shows the best performance according to *CORR* (0.93) and *RMSE* (2.85 °C) scores; however, the simulation with the WSM6 scheme and cumulus scheme turning off (Run5) ranks first according to *BIAS* (2.21 °C) scores. Analysis nudging (Run7) can further improve the model ability in reproducing temperature, with the best scores of *CORR* (0.97) and *RMSE* (1.03 °C) among all the sensitivity experiments.

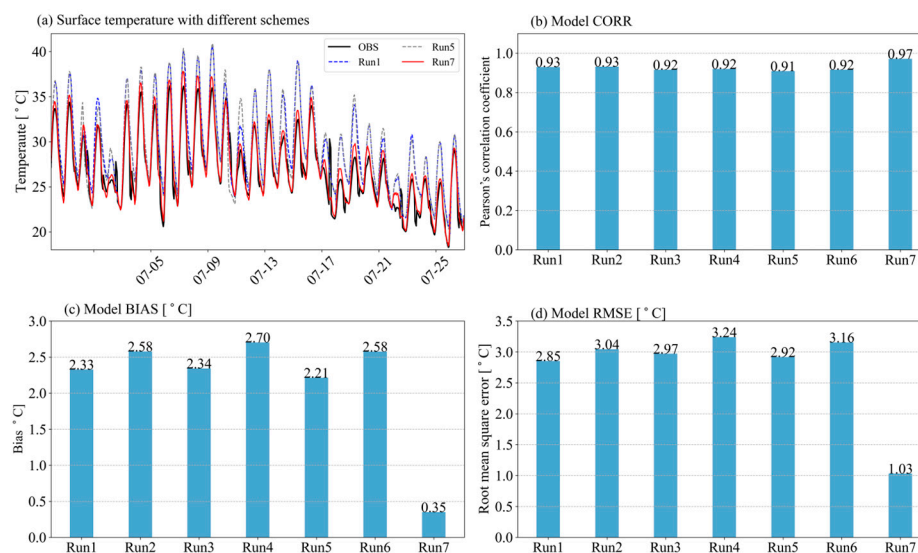


**Figure 8.** The time series of surface temperature averaged from all station observations, along with those from the corresponding sensitivity simulations (a) as well as the statistical scores of *CORR* (b), *BIAS* (c), and *RMSE* (d) for all the sensitivity experiments.

Precipitation can also be influenced by wind speed. Thus, the simulations of wind speed are also investigated. Figure 9 shows the spatial distribution of wind speed from the observation and model simulations, while WRF captures the spatial features of wind speed over Hebei Province. Overestimations are evident in the model simulations, particularly in the central regions of Hebei Province. For instance, many stations in the central regions record wind speeds of approximately 0.5 m/s, whereas the simulations indicate speeds around 2.5 m/s. The simulation with analysis nudging (Run7) shows better agreement with the observations, with much lower wind speed compared to other sensitivity experiments. Consequently, analysis nudging can further improve the model’s ability in reproducing wind speed.

Figure 10 shows the time series of observed wind speed as well as the corresponding statistical scores. The simulations generally reproduce the variation of wind speed. However, most simulations show large overestimation during all the simulation period, both at daytime and nighttime periods. Nevertheless, analysis nudging improves the model simulation significantly, with much lower wind speed compared to the other sensitivity experiments. For instance, the simulated wind speed of Run7 fits the observation very well during the periods of 1–10 July and 15–20 July. The time series of wind speed simulated by the parameterization schemes are quite similar, indicating similar model biases, ranging from 0.83 m/s to 0.96 m/s. The simulation with Kain–Fritsch and WSM6 (Run1) shows the best performance in terms of *BIAS* (0.83 m/s) and *RMSE* (1.07 m/s) scores, while the simulations with the Tiedtke scheme and Thompson scheme (Run4) and the Thompson scheme with the cumulus scheme turning off (Run6) show the best model performance according to *CORR* (0.73) scores. The simulation with analysis nudging (Run7) further improves the model performance, with much higher *CORR* (0.88) alongside lower *BIAS* (0.23 m/s) and *RMSE* (0.44 m/s) scores.

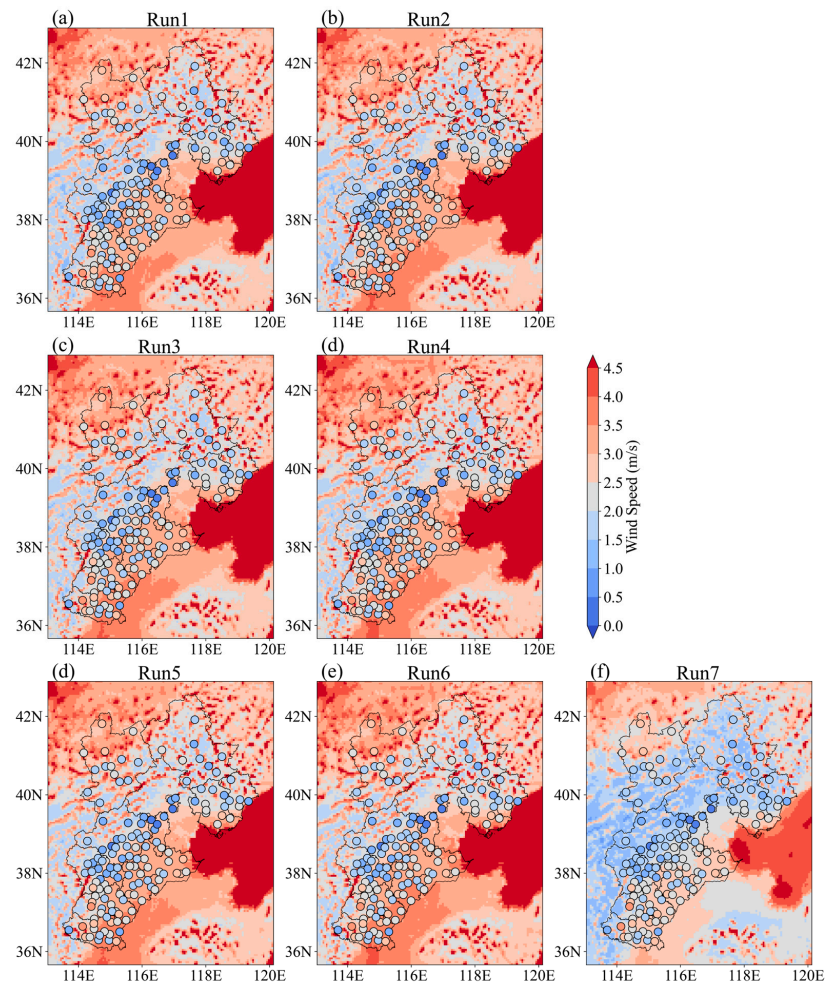


**Figure 9.** Comparison of daily mean wind speed in July 2017 between observations (colored dots) and sensitivity simulations (shadings). Units: m/s.

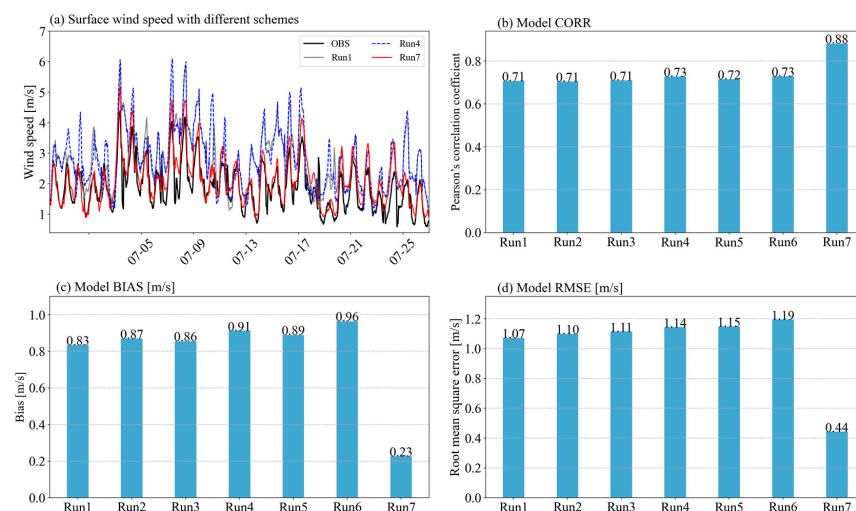


**Figure 10.** The time series of surface wind speed averaged of all station observations, along with those from the corresponding sensitivity simulations (a), as well as the statistical scores of CORR (b), BIAS (c) and RMSE (d) for all the sensitivity experiments.

#### 4. Discussion

As demonstrated in previous investigations over other regions, the performance of WRF in simulating precipitation is influenced by many factors, such as temperature, humidity, and wind, and the relationship among these variables is highly complicated. According to the Clausius–Clapeyron equation, precipitable water content will increase by 7% per degree of warming; however, many studies found that short-term duration precipitation does not increase proportionally [45,46]. In this study, for the parameterization scheme experiments, most sensitivity simulations underestimate precipitation over Hebei Province (Figure 3), which agrees with the negative bias of relative humidity (Figure 5), and thus, the bias in relative humidity may contribute to that of precipitation; however, it is also possible that the negative bias in relative humidity is caused by the underestimation of precipitation. Concurrently, the negative biases of relative humidity might also be influenced by temperature and wind speed, as the WRF model generally overestimates temperature (Figure 7) and wind speed (Figure 9), and the elevated temperatures and intensified wind speeds tend to increase the evaporation, leading to drier air and subsequently lower relative humidity.

It is evident that parameterization schemes significantly influence the model's performance in reproducing precipitation over Hebei Province, as well as temperature, relative humidity, and wind speed. Nonetheless, it is challenging to find the best parameterization scheme reproducing every precipitation event over Hebei Province well, as each scheme may be successful in reproducing one specific event while it fails in another. It is also challenging to find the best parameterization scheme for all the variables; for instance, the simulation with the Tiedtke and Thompson schemes shows the best performance in reproducing the average precipitation over Hebei Province, with the highest *CORR* and lowest *RMSE*, while the simulation with Kain–Fritsch and WSM6 ranks first among the experiments for the simulation of relative humidity. Thus, the determination of best parameterization schemes should rely on a systematic comparison of available combinations of parameterization schemes for a given location.

Moreover, other model configurations, such as analysis nudging, have a strong influence on model performance. In our study, the simulation with analysis nudging shows further improvement compared to the parameterization scheme experiments, indicating its advantage in precipitation simulations. Nevertheless, analysis nudging should be applied with caution, as it alters the dynamical balance by imposing external constraints on the evolution towards observational data. This can potentially impact the model's ability to simulate certain meteorological phenomena accurately, such as convective processes or boundary layer dynamics, particularly in high-resolution simulations.

It is worth noting that due to the availability of computational resources, the horizontal resolution is configured as 5 km, and the simulation periods of the sensitivity experiments cover only one month, which indicates the main limitation of this study. It is promising that the WRF model can generally reproduce the distribution of precipitation over Hebei Province well, which is consistent with previous studies over Asia or China [47,48]. However, the correlations between observed and simulated precipitation are approximately 0.3, which is relatively low compared with previous coarser resolution simulations; thus, further tuning on the physical parameterizations is needed in future work. Despite these limitations, this study is important to Hebei Province, as it provides valuable references for selecting the best model configurations for precipitation forecasting applications, and the availability of better high-resolution numerical simulations has potential for local hydrological simulation, which always requires high-resolution and reliable precipitation data.

#### 5. Conclusions

In this study, we investigate the influence of parameterization schemes and analysis nudging on precipitation simulation over Hebei Province using multiple month-long high-resolution WRF sensitivity simulations. The horizontal resolution of WRF is configured at 5 km, falling in the cumulus “gray-zone” category, which is seldom investigated in prior research. The performances of different parameterization schemes in reproducing

precipitation are analyzed using dense station observations recorded by the local Meteorology Administration as a reference. Additionally, further analysis was conducted on temperature, relative humidity, and wind speed to gain a comprehensive understanding of the model's ability and potential influencing processes associated with precipitation biases.

The sensitivity experiments indicate that the spatial and temporal distributions of precipitation in Hebei Province are well reproduced by the WRF model; however, the model tends to underestimate the precipitation compared with the observational data. The simulation with the Tiedtke cumulus parameterization scheme and Thompson microphysical parameterization scheme shows the best performance, with a *CORR* of 0.45 and *RMSE* of 0.34 mm/day; at the same time, the analysis nudging experiment, which assimilates the observational data, achieved a *CORR* of 0.47 and *RMSE* of 0.33 mm/day. Thus, the incorporation of observational data can improve the model performance, and it should be emphasized that the Tiedtke cumulus parameterization scheme combined with the Thompson microphysical parameterization scheme reach practically the same accuracy without analysis nudging as the sensitivity experiment with analysis nudging.

Further analysis indicates that the model bias in precipitation may be associated with biases in relative humidity, temperature, and wind speed, as the WRF model tends to underestimate the relative humidity, which will limit the precipitable water, thus consistent with the negative bias in precipitation. At the same time, WRF tends to overestimate temperature and wind speed, and the elevated temperatures and intensified wind speeds will increase the evaporation, resulting in the negative bias in relative humidity. However, further investigation into the detailed processes among these variables should be conducted in future research, which will be informative for the WRF model development.

It is noteworthy that no single scheme demonstrates optimal performance across all meteorological variables, and parameterization schemes possess individual advantages. Therefore, it is crucial to carefully select the most appropriate parameterization schemes for the WRF model in precipitation modeling and operational meteorological forecasting. The simulation with analysis nudging shows additional improvement compared to the parameterization scheme experiments, indicating its advantage in operational hydrological forecasting. However, caution should be paid in the application of analysis nudging, as it can break the dynamical balance by imposing external constraints on the evolution towards observational data.

**Author Contributions:** Conceptualization, Y.L. and E.Y.; methodology, E.Y.; software, X.C.; validation, Y.L., Z.T. and X.C.; formal analysis, Y.L. and E.Y.; investigation, Y.L. and X.C.; writing—original draft preparation, Y.L., X.C., X.S. and E.Y.; writing—review and editing, Y.L., X.C. and E.Y.; visualization, X.C. and E.Y.; funding acquisition, Y.L., Z.T. and E.Y. All authors have read and agreed to the published version of the manuscript.

**Funding:** This work was supported by the National Natural Science Foundation of China (42075168) and “Hebei Meteorological Information Center Meteorological Business Core Capability Enhancement Project”.

**Data Availability Statement:** Due to privacy the datasets generated during this study are available from the authors upon reasonable request.

**Acknowledgments:** We particularly thank the European Centre for Medium-Range Weather Forecasts for providing the ERA5 reanalysis data.

**Conflicts of Interest:** The authors declare no conflicts of interest.

## References

1. Rial, J.A.; Pielke, R.A.; Beniston, M.; Claussen, M.; Canadell, J.; Cox, P.; Held, H.; de Noblet-Ducoudré, N.; Prinn, R.; Reynolds, J.F.; et al. Nonlinearities, Feedbacks and Critical Thresholds within the Earth's Climate System. *Clim. Chang.* **2004**, *65*, 11–38. [[CrossRef](#)]
2. Steffen, W.; Richardson, K.; Rockström, J.; Schellnhuber, H.J.; Dube, O.P.; Dutreuil, S.; Lenton, T.M.; Lubchenco, J. The emergence and evolution of Earth System Science. *Nat. Rev. Earth Environ.* **2020**, *1*, 54–63. [[CrossRef](#)]
3. Thompson, P.D. A History of Numerical Weather Prediction in the United States. *Bull. Am. Meteorol. Soc.* **1983**, *64*, 755–769.

4. Dawson, A.; Palmer, T.N. Simulating weather regimes: Impact of model resolution and stochastic parameterization. *Clim. Dyn.* **2015**, *44*, 2177–2193. [[CrossRef](#)]
5. Dudhia, J. A history of mesoscale model development. *Asia-Pac. J. Atmos. Sci.* **2014**, *50*, 121–131. [[CrossRef](#)]
6. Miller, M.J.; Palmer, T.N.; Swinbank, R. Parameterization and influence of subgridscale orography in general circulation and numerical weather prediction models. *Meteorol. Atmos. Phys.* **1989**, *40*, 84–109. [[CrossRef](#)]
7. Palmer, T.N. A nonlinear dynamical perspective on model error: A proposal for non-local stochastic-dynamic parametrization in weather and climate prediction models. *Q. J. Roy. Meteor. Soc.* **2001**, *127*, 279–304. [[CrossRef](#)]
8. Phillips, T.J.; Potter, G.L.; Williamson, D.L.; Cederwall, R.T.; Boyle, J.S.; Fiorino, M.; Hnilo, J.J.; Olson, J.G.; Xie, S.; Yio, J.J. Evaluating Parameterizations in General Circulation Models: Climate Simulation Meets Weather Prediction. *Bull. Am. Meteorol. Soc.* **2004**, *85*, 1903–1916. [[CrossRef](#)]
9. Tiedtke, M. Representation of Clouds in Large-Scale Models. *Mon. Weather Rev.* **1993**, *121*, 3040–3061. [[CrossRef](#)]
10. Chen, X.; Pauluis, O.M.; Zhang, F. Regional simulation of Indian summer monsoon intraseasonal oscillations at gray-zone resolution. *Atmos. Chem. Phys.* **2018**, *18*, 1003–1022. [[CrossRef](#)]
11. Doubrawa, P.; Muñoz-Esparza, D. Simulating Real Atmospheric Boundary Layers at Gray-Zone Resolutions: How Do Currently Available Turbulence Parameterizations Perform? *Atmosphere* **2020**, *11*, 345. [[CrossRef](#)]
12. Taraphdar, S.; Pauluis, O.M.; Xue, L.; Liu, C.; Rasmussen, R.; Ajayamohan, R.S.; Tessendorf, S.; Jing, X.; Chen, S.; Grabowski, W.W. WRF Gray-Zone Simulations of Precipitation Over the Middle-East and the UAE: Impacts of Physical Parameterizations and Resolution. *J. Geophys. Res. Atmos.* **2021**, *126*, e2021JD034648. [[CrossRef](#)]
13. Zhang, X.; Yang, Y.; Chen, B.; Huang, W. Operational Precipitation Forecast Over China Using the Weather Research and Forecasting (WRF) Model at a Gray-Zone Resolution: Impact of Convection Parameterization. *Weather Forecast.* **2021**, *36*, 915–928. [[CrossRef](#)]
14. Zhou, P.; Shao, M.; Ma, M.; Ou, T.; Tang, J. WRF gray-zone dynamical downscaling over the Tibetan Plateau during 1999–2019: Model performance and added value. *Clim. Dyn.* **2023**, *61*, 1371–1390. [[CrossRef](#)]
15. Ma, M.; Ou, T.; Liu, D.; Wang, S.; Fang, J.; Tang, J. Summer regional climate simulations over Tibetan Plateau: From gray zone to convection permitting scale. *Clim. Dyn.* **2023**, *60*, 301–322. [[CrossRef](#)]
16. Sun, Y.; Yi, L.; Zhong, Z.; Hu, Y.; Ha, Y. Dependence of model convergence on horizontal resolution and convective parameterization in simulations of a tropical cyclone at gray-zone resolutions. *J. Geophys. Res. Atmos.* **2013**, *118*, 7715–7732. [[CrossRef](#)]
17. Xu, H.; Wang, H.; Duan, Y. An Investigation of the Impact of Different Turbulence Schemes on the Tropical Cyclone Boundary Layer at Turbulent Gray-Zone Resolution. *J. Geophys. Res. Atmos.* **2021**, *126*, e2021JD035327. [[CrossRef](#)]
18. Ou, T.; Chen, D.; Chen, X.; Lin, C.; Yang, K.; Lai, H.-W.; Zhang, F. Simulation of summer precipitation diurnal cycles over the Tibetan Plateau at the gray-zone grid spacing for cumulus parameterization. *Clim. Dyn.* **2020**, *54*, 3525–3539. [[CrossRef](#)]
19. Ramos-Valle, A.N.; Prein, A.F.; Ge, M.; Wang, D.; Giangrande, S.E. Grid Spacing Sensitivities of Simulated Mid-Latitude and Tropical Mesoscale Convective Systems in the Convective Gray Zone. *J. Geophys. Res. Atmos.* **2023**, *128*, e2022JD037043. [[CrossRef](#)]
20. Jeworrek, J.; West, G.; Stull, R. Evaluation of Cumulus and Microphysics Parameterizations in WRF across the Convective Gray Zone. *Weather Forecast.* **2019**, *34*, 1097–1115. [[CrossRef](#)]
21. Yu, E.; Bai, R.; Chen, X.; Shao, L. Impact of physical parameterizations on wind simulation with WRF V3.9.1.1 under stable conditions at planetary boundary layer gray-zone resolution: A case study over the coastal regions of North China. *Geosci. Model. Dev.* **2022**, *15*, 8111–8134. [[CrossRef](#)]
22. Han, J.-Y.; Hong, S.-Y.; Sunny Lim, K.-S.; Han, J. Sensitivity of a Cumulus Parameterization Scheme to Precipitation Production Representation and Its Impact on a Heavy Rain Event over Korea. *Mon. Weather Rev.* **2016**, *144*, 2125–2135. [[CrossRef](#)]
23. Yu, E.; Wang, H.; Gao, Y.; Sun, J. Impacts of cumulus convective parameterization schemes on summer monsoon precipitation simulation over China. *Acta Meteorol. Sin.* **2011**, *25*, 581–592. [[CrossRef](#)]
24. Kumar, R.A.; Dudhia, J.; Bhowmik, S.R. Evaluation of Physics options of the Weather Research and Forecasting (WRF) Model to simulate high impact heavy rainfall events over Indian Monsoon region. *G Eofizika* **2010**, *27*, 101–125.
25. Biswas, M.K.; Bernardet, L.; Dudhia, J. Sensitivity of hurricane forecasts to cumulus parameterizations in the HWRF model. *Geophys. Res. Lett.* **2014**, *41*, 9113–9119. [[CrossRef](#)]
26. Pennelly, C.; Reuter, G.; Flesch, T. Verification of the WRF model for simulating heavy precipitation in Alberta. *Atmos. Res.* **2014**, *135*, 172–192. [[CrossRef](#)]
27. Gelpi, I.R.; Gaztelumendi, S.; Carreño, S.; Hernández, R.; Egaña, J. Study of NWP parameterizations on extreme precipitation events over Basque Country. *Adv. Sci. Res.* **2016**, *13*, 137–144. [[CrossRef](#)]
28. Shepherd, T.J.; Walsh, K.J. Sensitivity of hurricane track to cumulus parameterization schemes in the WRF model for three intense tropical cyclones: Impact of convective asymmetry. *Meteorol. Atmos. Phys.* **2017**, *129*, 345–374. [[CrossRef](#)]
29. Guo, R.; Lin, Z.; Mo, X.; Yang, C. Responses of crop yield and water use efficiency to climate change in the North China Plain. *Agric. Water Manag.* **2010**, *97*, 1185–1194. [[CrossRef](#)]
30. Jeong, S.-J.; Ho, C.-H.; Piao, S.; Kim, J.; Ciais, P.; Lee, Y.-B.; Jhun, J.-G.; Park, S.K. Effects of double cropping on summer climate of the North China Plain and neighbouring regions. *Nat. Clim. Chang.* **2014**, *4*, 615–619. [[CrossRef](#)]
31. Wang, E.; Yu, Q.; Wu, D.; Xia, J. Climate, agricultural production and hydrological balance in the North China Plain. *Int. J. Climatol.* **2008**, *28*, 1959–1970. [[CrossRef](#)]

32. Skamarock, W.C.; Klemp, J.B.; Dudhia, J.; Gill, D.O.; Barker, D.M.; Duda, M.G.; Huang, X.-Y.; Wang, W.; Powers, J.G. A description of the advanced research WRF version 3. *NCAR Tech. Note* **2008**, *475*, 113.
33. Hersbach, H.; Bell, B.; Berrisford, P.; Hirahara, S.; Horányi, A.; Muñoz-Sabater, J.; Nicolas, J.; Peubey, C.; Radu, R.; Schepers, D.; et al. The ERA5 global reanalysis. *Q. J. Roy. Meteor. Soc.* **2020**, *146*, 1999–2049. [[CrossRef](#)]
34. Zhou, P.; Ma, M.; Shao, M.; Tang, J. Sensitivity of summer precipitation simulation to the physical parameterizations in WRF over the Tibetan Plateau: A case study of 2018. *Atmos. Res.* **2023**, *299*, 107174. [[CrossRef](#)]
35. Hong, S.-Y.; Lim, J.-O.J. The WRF single-moment 6-class microphysics scheme (WSM6). *Asia-Pac. J. Atmos. Sci.* **2006**, *42*, 129–151.
36. Thompson, G.; Field, P.R.; Rasmussen, R.M.; Hall, W.D. Explicit Forecasts of Winter Precipitation Using an Improved Bulk Microphysics Scheme. Part II: Implementation of a New Snow Parameterization. *Mon. Weather. Rev.* **2008**, *136*, 5095–5115. [[CrossRef](#)]
37. Kain, J.S. The Kain–Fritsch Convective Parameterization: An Update. *J. Appl. Meteorol.* **2004**, *43*, 170–181. [[CrossRef](#)]
38. Tiedtke, M. A Comprehensive Mass Flux Scheme for Cumulus Parameterization in Large-Scale Models. *Mon. Weather. Rev.* **1989**, *117*, 1779–1800. [[CrossRef](#)]
39. Stauffer, D.R.; Seaman, N.L. Multiscale Four-Dimensional Data Assimilation. *J. Appl. Meteorol. Clim.* **1994**, *33*, 416–434. [[CrossRef](#)]
40. Hong, S.-Y.; Noh, Y.; Dudhia, J. A new vertical diffusion package with an explicit treatment of entrainment processes. *Mon. Weather. Rev.* **2006**, *134*, 2318–2341. [[CrossRef](#)]
41. Mlawer, E.J.; Taubman, S.J.; Brown, P.D.; Iacono, M.J.; Clough, S.A. Radiative transfer for inhomogeneous atmospheres: RRTM, a validated correlated-k model for the longwave. *J. Geophys. Res. Atmos.* **1997**, *102*, 16663–16682. [[CrossRef](#)]
42. Dudhia, J. Numerical study of convection observed during the winter monsoon experiment using a mesoscale two-dimensional model. *J. Atmos. Sci.* **1989**, *46*, 3077–3107. [[CrossRef](#)]
43. Niu, G.; Yang, Z.; Mitchell, K.E.; Chen, F.; Ek, M.B.; Barlage, M.; Kumar, A.; Manning, K.; Niyogi, D.; Rosero, E. The community Noah land surface model with multiparameterization options (Noah-MP): 1. Model description and evaluation with local-scale measurements. *J. Geophys. Res. Atmos.* **2011**, *116*, D12109. [[CrossRef](#)]
44. Yang, Z.; Niu, G.; Mitchell, K.E.; Chen, F.; Ek, M.B.; Barlage, M.; Longuevergne, L.; Manning, K.; Niyogi, D.; Tewari, M. The community Noah land surface model with multiparameterization options (Noah-MP): 2. Evaluation over global river basins. *J. Geophys. Res. Atmos.* **2011**, *116*, D12110. [[CrossRef](#)]
45. Wang, H.; Sun, F.; Liu, W. The Dependence of Daily and Hourly Precipitation Extremes on Temperature and Atmospheric Humidity over China. *J. Clim.* **2018**, *31*, 8931–8944. [[CrossRef](#)]
46. Betts, A.K.; Desjardins, R.; Worth, D.; Beckage, B. Climate coupling between temperature, humidity, precipitation, and cloud cover over the Canadian Prairies. *J. Geophys. Res. Atmos.* **2014**, *119*, 13305–13326. [[CrossRef](#)]
47. Liu, D.; Yang, B.; Zhang, Y.; Qian, Y.; Huang, A.; Zhou, Y.; Zhang, L. Combined impacts of convection and microphysics parameterizations on the simulations of precipitation and cloud properties over Asia. *Atmos. Res.* **2018**, *212*, 172–185. [[CrossRef](#)]
48. Gao, S.; Huang, D.; Du, N.; Ren, C.; Yu, H. WRF ensemble dynamical downscaling of precipitation over China using different cumulus convective schemes. *Atmos. Res.* **2022**, *271*, 106116. [[CrossRef](#)]

**Disclaimer/Publisher’s Note:** The statements, opinions and data contained in all publications are solely those of the individual author(s) and contributor(s) and not of MDPI and/or the editor(s). MDPI and/or the editor(s) disclaim responsibility for any injury to people or property resulting from any ideas, methods, instructions or products referred to in the content.